A Study on the Electrodeposition of NiFe Alloy Thin Films Using Chronocoulometry and Electrochemical Quartz Crystal Microgravimetry

Noseung Myung

Department of Applied Chemistry, Konkuk University Chungju Campus, Chungju, Chungbuk 380-701, Korea
Received May 25, 2001

Ni, Fe and NiFe alloy thin films were electrodeposited at a polycrystalline Au surface using a range of electrolytes and potentials. Coulometry and EQCM were used for real-time monitoring of electroplating efficiency of the Ni and Fe. The plating efficiency of NiFe alloy thin films was computed with the aid of ICP spectrometry. In general, plating efficiency increased to a steady value with deposition time. Plating efficiency of Fe was lower than that of Ni at −0.85 and −1.0 V but the efficiency approached to the similar plateau value to that of Ni at more negative potentials. The films with higher content of Fe showed different stripping behavior from the ones with higher content of Ni. Finally, compositional data and real-time plating efficiency are presented for films electrodeposited using a range of electrolytes and potentials.

Keywords : Electrodeposition, NiFe alloy, EQCM, Chronocoulometry.

Introduction

NiFe alloys ranging in composition from the Ni-rich Permalloy to the Fe-rich Invar have a variety of high technology applications due to their wide spectrum of physical properties.[1,2] For example, Permalloy has found use in memory devices due to magnetic properties and Invar exhibiting a low thermal expansion coefficient has many applications such as watch springs, laser housings and space technology. Also, NiFe alloy coatings can be used as decorative and protective materials.

Among the several methods, electrodeposition has proven to be an efficient process for the synthesis of NiFe alloy films due to flexibility, low cost and capability of being used for parts with any size and geometry.[3-6] In addition, electrodeposition of NiFe alloys has attracted considerable attention because it exhibits the phenomenon of "anomalous codeposition".[1-4,6] This term introduced by Brenner is being used to describe the preferential deposition of the less noble metal, Fe, to the more noble metal, Ni.[1,2] In other words, the reduction of nickel is inhibited while the deposition of iron is enhanced when compared with their individual deposition rates. Several attempts have been made to explain the anomalous codeposition of NiFe alloys. However, the focus of this paper is not on the elucidation of anomalous codeposition.

The magnetic, mechanical and corrosion properties of NiFe alloys are affected by a number of factors including roughness, grain size and alloy composition. In turn, these factors are dependent on deposition conditions such as electrolyte composition, pH, applied current density and agitation.[7-9]

In this report, the effects of the applied potential and electrolyte concentration on the composition of the NiFe alloy films are explored *via* electrochemical quartz crystal microgravimetry (EQCM), chronocoulometry, Auger and inductively coupled plasma (ICP) spectrometry. Especially, EQCM combined with coulometry is described for real-time monitoring of the deposition efficiencies of Ni and Fe, which has not been reported before. Also, the plating efficiency of NiFe alloy thin films was computed with the aid of ICP spectrometry.

Experimental Section

An EG&G PAR 263A system equipped with Model M250/270 electrochemistry software was used. The EQCM (Seiko EG&G Model QCA 917) consisted of an oscillator module (QCA 917-11) and a 9 MHz AT-cut Au crystal (geometric area, 0.2 cm^2). The electrodeposited alloy thin film was anodically stripped in a blank solution and subsequently analyzed for Ni and Fe content by a Perkin Elmer ICP spectrometry (Model Optima 2000 DV). Auger depth profile was obtained with a VG Model ESCALAB 210.

All chemicals were purchased from Aldrich and used as received. All electrolytes were prepared with double-distilled water (Corning-Megapure) and purged with ultrapure N_2. The 0.1 *M* Ni (or 0.1 *M* Fe) electrolyte for Ni (or Fe) electrodeposition was prepared with 0.1 *M* $NiSO_4$ (or 0.1 *M* $FeSO_4$) + 0.35 *M* Na_2SO_4 + 0.2 *M* H_3BO_3. NiFe alloy films were electrosynthesized at several potentials from 0.1 *M* $NiSO_4$ + 0.1 *M* $FeSO_4$ + 0.25 *M* Na_2SO_4 + 0.2 *M* H_3BO_3 (100 m*M* Fe solution) and 0.1 *M* $NiSO_4$ + 5 m*M* $FeSO_4$ + 0.35 *M* Na_2SO_4 + 0.2 *M* H_3BO_3 (5 m*M* Fe solution). The pH of all electrolytes was adjusted to 3.0 with 0.1 *M* H_2SO_4.[3] The pH and composition of electrolytes were selected based on previous works.[2-4,9]

The electrochemical cell was custom built with plexiglass and consisted of a gold working electrode, a Pt auxiliary electrode, and an Ag/AgCl/3 *M* NaCl reference electrode. Prior to the electrodeposition experiments, the quality of the gold electrode surface was checked by cyclic voltammograms (CVs) in 0.1 *M* H_2SO_4.[10] The potential was cycled between −0.8 and 0.7 V until voltammetric and frequency signals

were stable. The data represented below are average values of at least three replicate runs.

Results and Discussion

Due to several advantages, the EQCM technique has been applied to studies of metals and alloy systems such as Ni, Cu, CuNi, FeCr and CdSe.[11-15] However, EQCM has not been applied to the study of the NiFe system, yet. Especially, *in-situ* and real-time monitoring of electrodeposition efficiency is possible by coupling the EQCM technique with coulometry. For example, composition of CdSe thin film was continuously monitored from the charge and mass changes during the film growth via combined coulometry and EQCM.[11]

Figure 1 shows representative coulometry and EQCM traces for 0.1 *M* Ni (A) and 0.1 *M* Fe (B) solutions at 1.0 V. As shown in the Figure, significant Ni deposition occurred after 10 s and Fe deposition after 50 s. That is, Ni deposition is significantly faster than Fe at this potential. From combination of the frequency change (mass increase) and Faradays law, the charge consumed for Ni deposition can be calculated. For example, the charge (Q) and frequency change (Δf) during the electrodeposition of Ni can be connected via the Faraday's law and the Sauerbrey equation:[17]

$$\Delta m = -k\Delta f \quad (1)$$

$$Q = nFN \quad (2)$$

$$Q = -(nF\,k/M)\,\Delta f \quad (3)$$

In equations (1)-(3), Δm is the mass of the deposit, n is the electron stoichiometry, F is the Faraday constant, N is the number of moles deposited, and k is the sensitivity factor. Finally, M is the molar mass of the deposit. As compared with a coulometric measurement, the charge affords plating efficiency for Ni deposition during the film growth. Plating efficiencies thus obtained for Ni (—) and Fe (---) are shown in Figure 2 as a function of deposition potential and time. The coulombic efficiency of Ni increases with time and decreasing potential. The efficiency continues to increase with deposition time at −0.85 V, but it approaches to the steady value of 70-80% at more negative potentials and the residual charge is attributed to the proton reduction.[10,12,13] These values are in good agreement with the previous results.[13] In contrast to the Ni system, deposition of Fe does not significantly occur and the coulombic efficiency is very small at −0.85 and −1.0 V. At more negative potentials, the efficiency increases with time and approaches to a plateau value. This Figure clearly demonstrates that the deposition

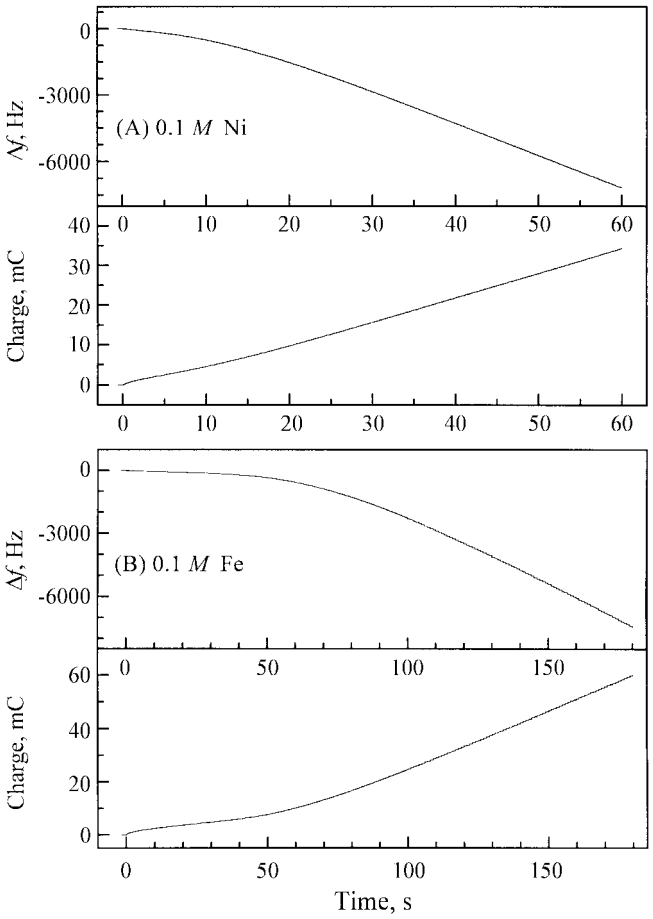

Figure 1. Representative combined coulometric and microgravimetric traces for the electrodeposition of a film at 1.0 V in the 0.1 *M* Ni (A) and 0.1 *M* Fe (B) electrolyte. (see experimental section for details)

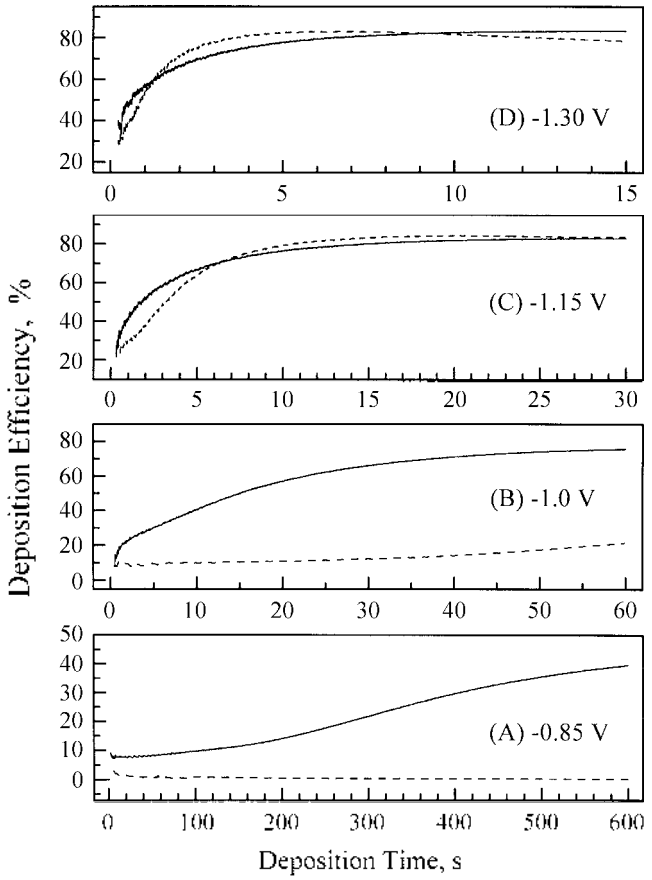

Figure 2. Deposition efficiency of Ni (—) and Fe (---) as a function of time and deposition potential. Same electrolyte conditions as in Figure 1

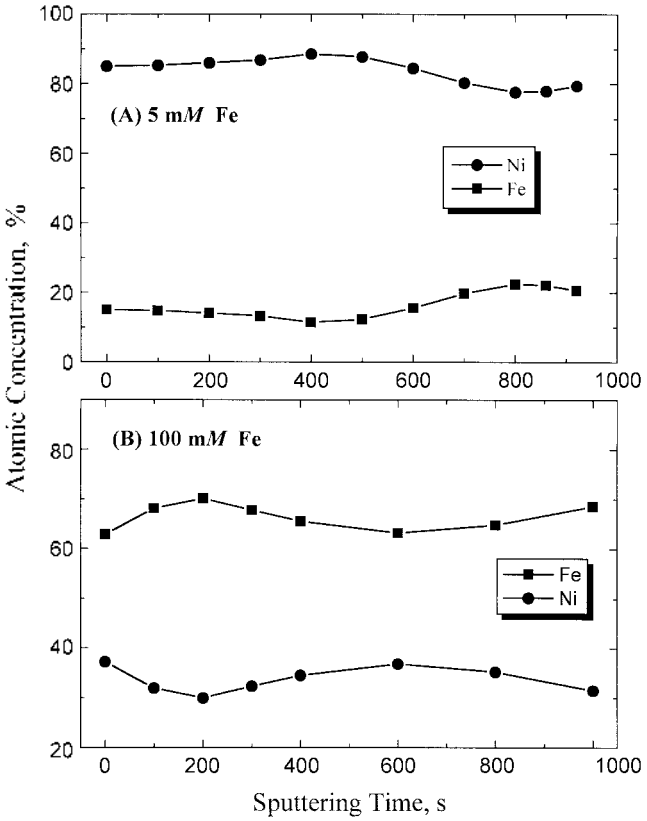

Figure 3. Auger depth profile of a film deposited at −1.0 V using (A) 5 m*M* Fe and (B) 100 m*M* Fe solution.

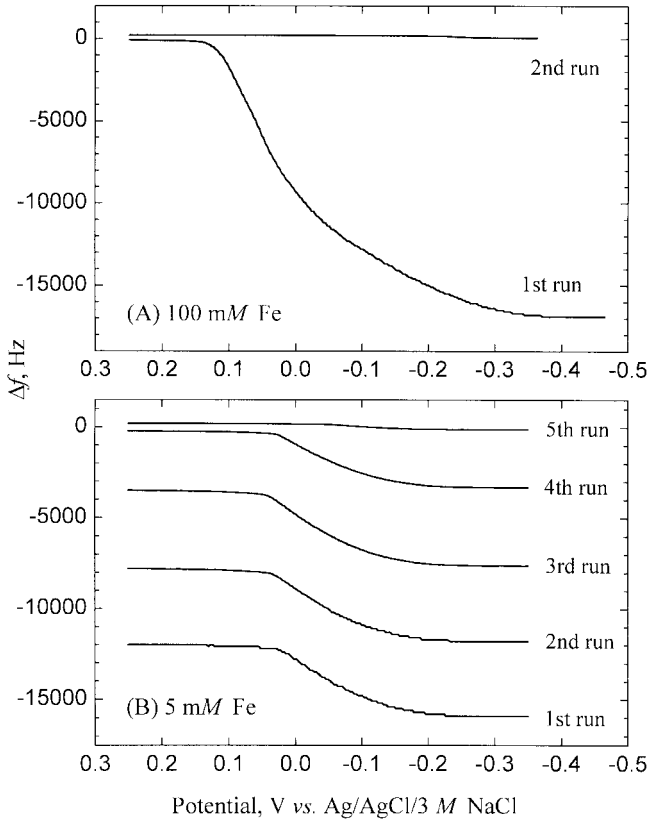

Figure 4. Frequency changes during the stripping voltammetry for the films deposited in (A) 100 m*M* Fe and (B) 5 m*M* Fe solution at −1.15 V. Sweep rate: 20 mV/s.

efficiency is not fixed but changed with time. Therefore, deposition time as well as potential should be considered to describe the plating efficiency. From the Figures 1 and 2, it is shown that there are two different stages during the electrodeposition: initial slow deposition and lower efficiency, followed by fast deposition and higher efficiency. The difference can be attributed to the different deposition kinetics depending on the layers (*e.g.*, monolayer or multilayer).[10]

To investigate composition modulation of the NiFe thin film depending on the deposition time and therefore depth, Auger depth profile of a thin film was obtained (Figure 3). A film deposited at −1.0 V using a 5 m*M* Fe solution (see experimental section) shows higher content of Ni and no distinctive difference in composition with depth. Also, a film deposited at −1.0 V using a 100 m*M* Fe solution shows the same trend except higher content of Fe. This Figure indicates that Ni-rich or Fe-rich NiFe alloy thin films can be obtained by controlling the electrolyte composition.

Since the stripping voltammetry of NiFe alloy thin film yields only one peak and no separate peaks for Ni and Fe, it is not possible to differentiate the content of Ni from the other in NiFe alloy thin films using stripping voltammetry.[5,9,16] Therefore, compositional analysis was conducted with ICP spectrometry to determine the deposition efficiency through the alloy composition. For ICP measurements, alloy thin films deposited with different electrolytes at various potentials were electrochemically stripped in a blank solution.

Interestingly enough, Figure 4 shows distinctively different stripping behavior of two alloy films. Figure 4(A) shows the frequency change during the anodic stripping voltammetry for the film deposited at −1.15 V using a 100 m*M* Fe solution. Note that the film was almost completely stripped in the first sweep. On the other hand, a film deposited using a 5 m*M* Fe solution at the same potential, 4 sweeps were needed to strip the NiFe alloy film (Figure 4(B)). This difference could be attributed to the higher content of Fe in the film deposited using a 100 m*M* Fe solution. It is also worthy of note that every run shows the same frequency change of *ca.* 4 KHz in Figure 4 (B).

Figure 5 shows the effects of applied potentials and electrolyte on the NiFe alloy composition obtained from the ICP analysis. It is clearly shown that alloy composition is sensitive to the applied potential as well as the plating bath. Especially, drastic change in alloy composition can be achieved by varying the electrolyte composition. Therefore, a fine tuning of composition might be possible through the combination of potential and electrolyte control. Also shown is that the weight ratio of Ni/Fe in the alloy film is not same as the concentration ratio of Ni/Fe in the electrolyte. For example, the weight of Fe deposited is 1.7 times higher that that of Ni whereas the electrolyte contains equal amount of Ni^{2+} and Fe^{2+} ions (−1.0 V in Figure 5(A)). This "anomalous codeposition" is shown in Figure 5(B) again when the Fe concentration is decreased to 20 times lower than that of Ni.

Finally, the plating efficiency with deposition time was

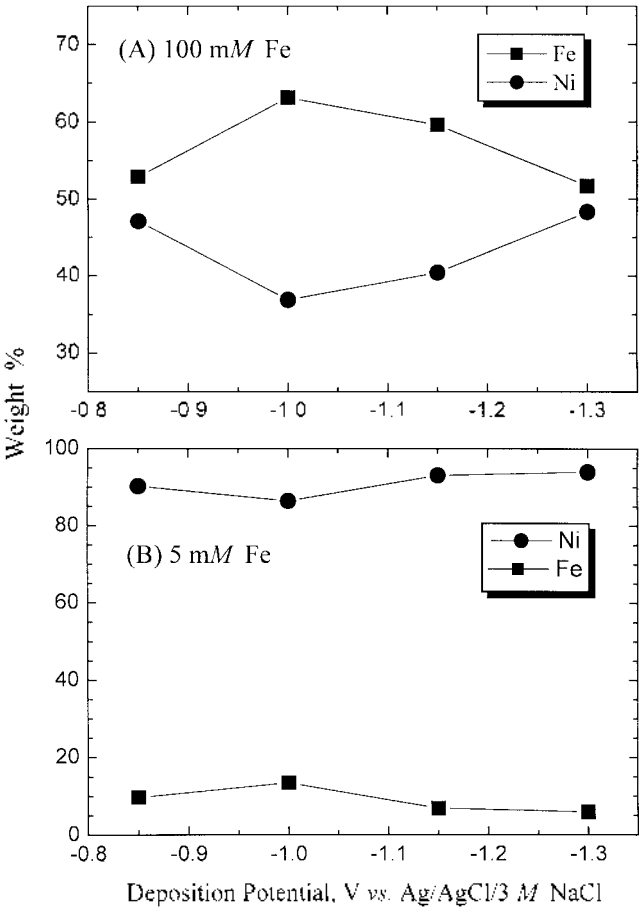

Figure 5. Dependence of NiFe film composition on the electrodeposition potential. Plating bath: (A) 100 m*M* Fe solution (B) 5 m*M* Fe solution.

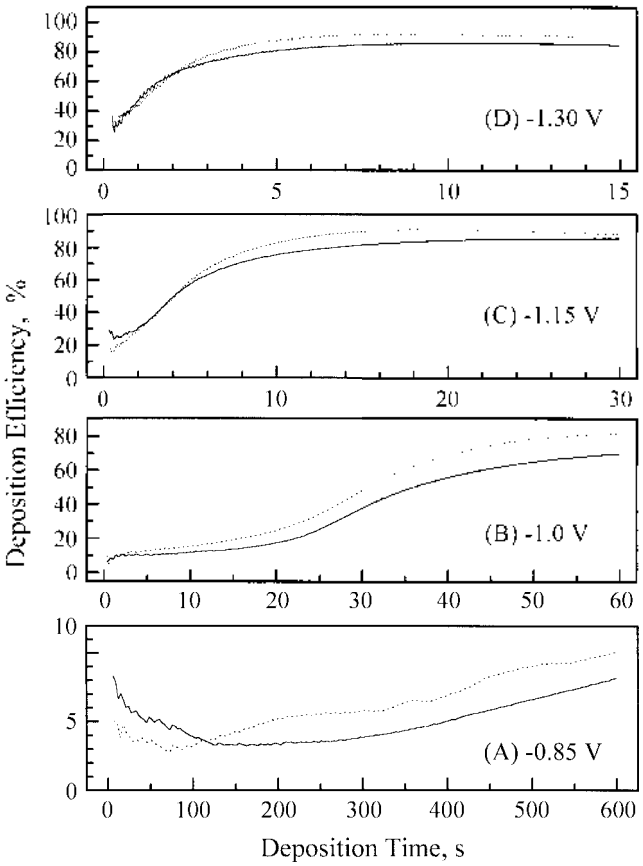

Figure 6. Deposition efficiency of NiFe alloy thin films as a function of time and deposition potential. (—): 5 m*M* Fe solution and (---): 100 m*M* Fe solution.

computed with the aid of the ICP analysis data in Figure 5 for the alloy thin films as a function of deposition potential and electrolyte composition. In this case, the composition of Ni and Fe can not be determined separately via combined EQCM and coulometry since EQCM is not chemical species selective.[11] Therefore, ex situ ICP spectrometry and assumption that there is no distinctive difference in composition with depth were adopted to calculate the deposition efficiencies. First, the charge consumed for Ni and Fe deposition was calculated from the ICP results and Faradays law. Then, comparison of the charge for Ni and Fe thus calculated with the total charge for the electrodeposition allows mapping of the plating efficiency as a function of potential and electrolyte in a manner similar to Figure 2. The results are shown in Figure 6. As shown, films deposited using a 100 m*M* Fe solution shows slightly higher plating efficiency at all potentials. Also, deposition rate observed from the frequency change during the plating was much faster for the 100 m*M* Fe solution than the 5 m*M* Fe solution (not shown).

In summary, combined use of coulometry and EQCM affords a route to real-time monitoring of plating efficiency of Ni and Fe. The plating efficiency of NiFe alloy thin films was computed with the aid of ICP spectrometry. This study has shown that alloy composition can be tuned by varying the plating potential as well as bath conditions. Also shown is that electrolyte composition is more effective to change the composition of NiFe alloy thin films than the deposition potential. Finally, different stripping behavior of alloy films with different composition has been demonstrated.

Acknowledgment. This work was supported by Korea Research Foundation Grant (KRF-99-015-DP0259). The author is grateful to Professor Jae-Gwang Lee for helpful discussion and Nam Hoon Kim at Perkin Elmer Korea for ICP analysis.

References

1. Andricacos, P. C.; Romankiw, L. T. In *Advances in Electrochemical Science and Engineering*; Gerisher, H., Tobias, C. H., Eds.; VCH: New York, U. S. A., 1994, Vol. 3, p 26.
2. Djokic, S. S.; Maksimovic, M. D. In *Modern Aspects of Electrochemistry*; Bockris, J. O. M., Conway, B. E., White, R. E., Eds; Plenum Press: New York, U.S.A., 1992, No. 22, 417.
3. Harris, T. M.; Wilson, J. L.; Bleakley, M. *J. Electrochem. Soc.* **1999**, *146*, 1461.
4. Grimmett, D. L.; Schwartz, M.; Nobe, K. *J. Electrochem. Soc.* **1990**, *137*, 3414.
5. Andricacos, P. C.; Romankiw, L. T. *J. Electrochem. Soc.* **1988**, *135*, 1172.
6. Dahms, H.; Croll, I. M. *J. Electrochem. Soc.* **1965**, *112*,

771.
7. Kieling, V. C. *Surf. Coat. Technol.* **1997**, *96*, 135.
8. Takai, M.; Kageyama, K.; Takefusa, S.; Nakamura, A.; Osaka, T. *IEICE Trans. Electron.* **1995**, *E78-C*, 1530.
9. Andricacos, P. C.; Arana, C.; Tabib, J.; Dukovic, J.; Romankiw, L. T. *J. Electrochem. Soc.* **1989**, *136*, 1336.
10. Lachenwitzer, A.; Magnussen, O. M. *J. Phys. Chem. B* **2000**, *104*, 7424.
11. Myung, N.; Wei, C.; Rajeshwar, K. *J. Electroanal. Chem.* **1993**, *356*, 281.
12. Zhou, M.; Myung, N.; Chen, X.; Rajeshwar, K. *J. Electroanal. Chem.* **1995**, *398*, 5.
13. Arkam, C.; Bouet, V.; Gabrielli, C.; Maurin, G.; Perrot, H. *J. Electrochem. Soc.* **1994**, *141*, L103.
14. Juzeliunas, E.; Pickering, H. W.; Weil, K. G. *J. Electrochem. Soc.* **2000**, *147*, 1088.
15. Schumutz, P.; Landolt, D. *Electrochim. Acta* **1999**, *45*, 899.
16. Zhou, M.; Myung, N.; Rajeshwar, K. *Electroanalysis* **1996**, *8*, 1140.
17. Myung, N.; Jun, J. H.; Ku, H. B.; Chung, H.-K.; Rajeshwar, K. *Microchem. J.* **1999**, *62*, 15.